HYSTERETIC RESTORING FORCE CHARACTERISTICS OF UNBONDED PRESTRESSED CONCRETE FRAMED STRUCTURE UNDER EARTHQUAKE LOAD

M. Nishiyama, H. Mugurama and F. Watanabe*

SUMMARY

An analytical method, by which hysteretic restoring force characteristics of unbonded prestressed concrete framed structure can be statically pursued on the basis of material properties, is presented. The bond-slip relationship between concrete and prestressing tendon is taken into account, and thus the method covers unbonded members and bonded members. For verifying the propriety of the analytical method, the experiment is carried out on a portal frame with an unbonded prestressed concrete beam of 4.2 m in length and reinforced concrete columns of 1 m in height. High intensity reversed cyclic lateral loading is applied. The experimental results show a good agreement with the analytical ones in terms of load-deflection relation and the fluctuation of the tendon stress at anchorage end.

Editors Note: This paper was first published in the Proceedings of the 1988 Pacific Concrete Conference and is reprinted with the permission of the Cement and Concrete Association of New Zealand and the New Zealand Concrete Society.

INTRODUCTION

In seismic areas, the application of unbonded prestressed concrete to primarily earthquake resistant members is prohibited due to several reasons, i.e. safety of tendon anchorage assembly against cyclic earthquake load, uncertainties with regard to the fluctuation of tendon stress, little available data on hysteretic restoring force characteristics and complexity in analysis, etc. However, unbonded prestressed concrete members can be very useful to develop the further demand for prestressed concrete structures, because of economical advantage of unbonded tendon, that is, no need for grouting at the construction site, and of practically perfect protection against corrosion comparing with the grouting which is likely to be imperfect. In addition, the past researches reported that small amounts of additional nonprestressed reinforcement can improve the restoring force characteristics and the flexural ductility [1,4].

In this study, an analytical method, by which hysteretic restoring force characteristics of unbonded prestressed concrete members and framed structures can be statically pursued on the basis of material properties, is presented. In this method, a structural member is divided into several blocks along member axis and each block is further subdivided into layers, which reflect mechanical properties of the materials. The stiffness matrix of the member is derived from these segments based on the assumptions that stresses and strains are constant in a segment and the cross section of the member remain plane after loading. The bond-slip relationship between concrete and prestressing tendon is taken into account, and thus, this method covers unbonded members and bonded members.

For verifying the propriety of the analytical method, the experiment is carried out on a portal frame with an unbonded prestressed concrete beam of 4.2 m in length and reinforced concrete columns of 1 m in height. High-intensity reversed cyclic loading is statically applied. The experimental results are compared with analytical results in terms of lateral load - deflection relation and the fluctuation of tendon stress at the anchorage end.

GENERAL DESCRIPTION OF ANALYTICAL METHOD

For the purpose of numerical calculation, a structural member is divided into several blocks in the direction of the longitudinal member axis and each block is further subdivided into layers. This method is called "Layer Element Method" and it has been developed by many researchers. In this study, the following are assumed:

1) Stress and strain are constant in a layer element.

2) The cross section of the member remains plane after loading, i.e., the longitudinal strain in concrete and the nonprestressed reinforcement is proportional to the distance from the neutral axis.

*Kyoto University, Japan.

3) Shear deformation is not taken into consideration. Although shear deformation is undoubtedly important in the case of the column, here the bending and axial force are assumed to dominate the deformation of the member.

4) The linear bond-slip relation between concrete and prestressing tendon is assumed.

5) Assumed stress-strain relation of concrete and reinforcement are proposed by Kent and Park [2], and Park, Kent and Sampson [5].

Bond Stress and Slip between Reinforcement and Concrete

Increment of bond stress between (j-1)-th block and j-th block ($\Delta\tau_j$) is calculated by the following equation.

$$\Delta\tau_j = \frac{2(\Delta_s P_{j-1} - \Delta_s P_j)}{\phi_s(l_{j-1} + l_j)} \tag{1}$$

where, $\Delta_s P_j$ = force increment of reinforcement in j-th block, ϕ_s = nominal surface area of a bar of unit length, and l_j = length of j-th block. $\Delta\tau_j$ is also expressed by bond-slip relationship ($\Delta\tau_j$ - ΔS_j), as follows,

$$\Delta\tau_j = K_j \cdot \Delta S_j \tag{2}$$

where, K_j = tangential modulus of bond-slip relation. In this study, K_j is assumed to be constant during loading.

The System of Linear Equations of Increments of Slip

The method used here was proposed by Kosaka et al. [3]. Dividing the member in the longitudinal direction into block elements $i = 1,2,\ldots,j,\ldots$ of length l_j, as shown in Fig. 1, the longitudinal strain increment of reinforcement $\Delta_s\varepsilon_j$, the concrete strain increment $\Delta_c\varepsilon_j$ and the increment of slip in unit length $\Delta_b\varepsilon_j$ are calculated by compatibility of displacements as follows,

$$\Delta_s\varepsilon_j = (\Delta u_{j+1} - \Delta u_j)/l_j \tag{3}$$

$$\Delta_c\varepsilon_j = (\Delta v_{j+1} - \Delta v_j)/l_j \tag{4}$$

$$\begin{aligned}\Delta_b\varepsilon_j &= (\Delta S_{j+1} - \Delta S_j)/l_j \\ &= (\Delta v_{j+1} - \Delta v_j)/l_j \\ &\quad - (\Delta u_{j+1} - \Delta u_j)/l_j\end{aligned} \tag{5}$$

where, S_j = slip between concrete and reinforcement, u_j and v_j = displacements of reinforcement and concrete. Therefore,

$$\begin{aligned}\Delta_s\varepsilon_j &= \Delta_c\varepsilon_j - \Delta_b\varepsilon_j \\ &= \Delta_c\varepsilon_j - (\Delta S_{j+1} - \Delta S_j)/l_j\end{aligned} \tag{6}$$

From the equilibrium of forces, we get the relationship between the stress of reinforcement and slip as below,

at the end 1 of member, as shown in Fig. 2;

$$-E_{s1}\cdot\Delta_c\varepsilon_1 = \left(\frac{E_{s1}}{l_1} + \frac{pK_1}{A_s}\right)\Delta_p S_1 - \frac{E_{s1}}{l_1}\Delta S_2 \tag{7}$$

between the ends;

$$\begin{aligned}E_{sj-1}\cdot\Delta_c\varepsilon_{j-1} - E_{sj}\cdot\Delta_c\varepsilon_j &= \frac{E_{sj-1}}{l_{j-1}}\Delta S_{j-1} \\ &+ \left(\frac{E_{sj-1}}{l_{j-1}} + \frac{E_{sj}}{l_j} + \frac{K_j\phi_s(l_{j-1} + l_j)}{2A_s}\right)\Delta S_j \\ &- \frac{E_{sj}}{l_j}\Delta S_{j+1}\end{aligned} \tag{8}$$

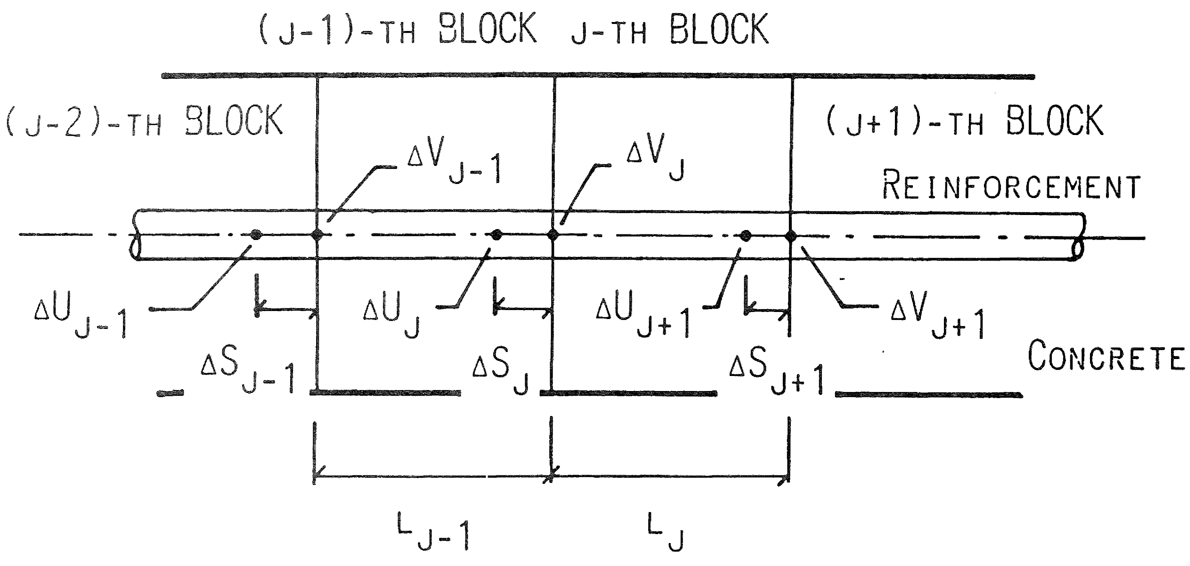

FIGURE 1 - COMPATIBILITY OF DISPLACEMENTS IN THE MEMBER

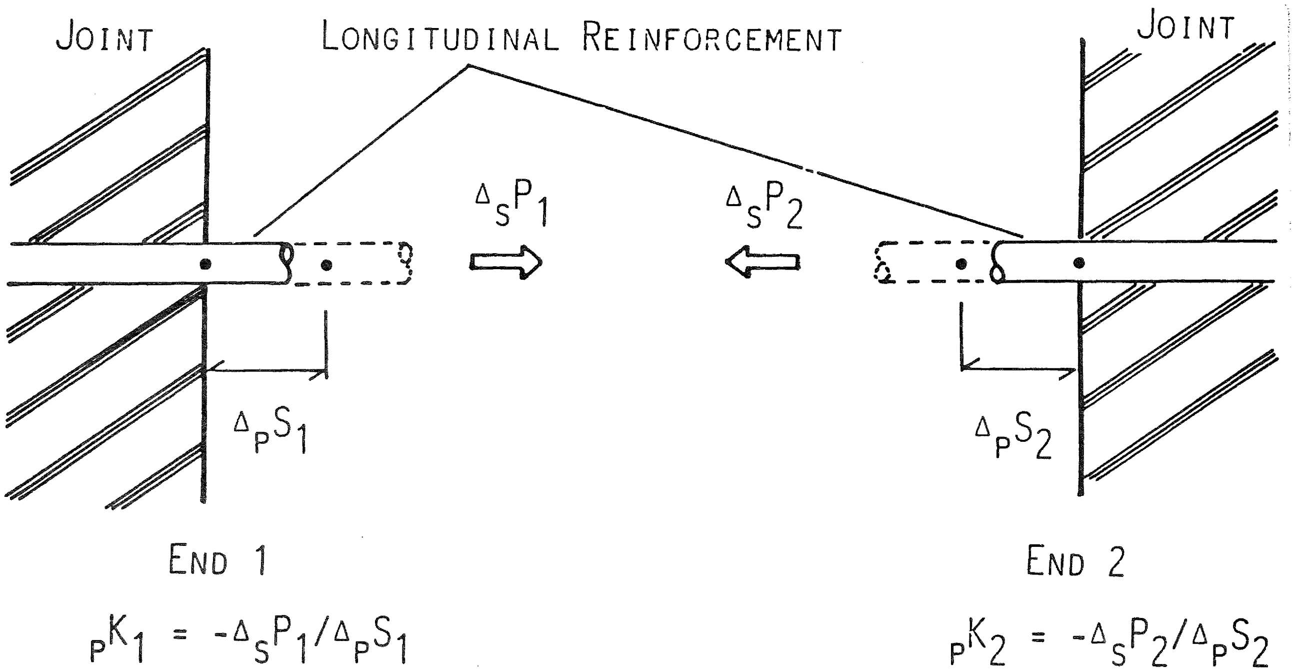

FIGURE 2 - FORCE AND SLIP INCREMENT OF REINFORCEMENT AT THE ENDS OF THE MEMBER

at the end 2 of member, as shown in Fig. 2;

$$E_{sn}\cdot\Delta_c\varepsilon_n = -\frac{E_{sn}}{l_n}\,\Delta S_n + \left(\frac{E_{sn}}{l_n} + \frac{{}_pK_2}{A_s}\right)\,\Delta_p S_2 \tag{9}$$

where, E_{sj} and A_s = tangential modulus and cross sectional area of reinforcement, $_pK_1 = -\Delta_s P_1/\Delta_p S_1$, $\Delta_p K_2 = \Delta_s P_2/\Delta_p S_2$, $\Delta_s P_1$ and $\Delta_s P_2$ = force increment of the reinforcement, $\Delta_p S_1$ and $\Delta_p S_2$ = slip increment of reinforcement at the ends of the member. Although $_pK_1$ and $_pK_2$ should be determined by some calculation, in this study because of simplification it is assumed that they are constant and large enough to restrain the tendon from coming out from the joint. This could be justified because the prestressing tendon was anchored almost perfectly on the steel plate.

These equations (7-9) represent the system of linear equation of ΔS_j . Increments of slip (ΔS_j) can be determined by given $\Delta_c\varepsilon_j$ (strain increment of concrete element located at the reinforcement level).

Substituting the calculated values of S_j into Eq. 5, we get $\Delta_b\varepsilon_j$. Stress increment of reinforcement $\Delta_s\sigma_j$ are calculated by

$$\begin{aligned}\Delta_s\sigma_j &= E_{sj}\,\Delta_s\varepsilon_j \\ &= E_{sj}\,\Delta_c\varepsilon_j - E_{sj}\,\Delta_b\varepsilon_j\end{aligned} \tag{10}$$

Derivation of the Stiffness Matrix of the Cross Section

The cross section of the member is subdivided in the z-direction into layers i = 1,2,...,m of cross-sectional areas A_{ij} and centroidal coordinates Z_{ij} . Centroidal coordinates of longitudinal steel reinforcement in j-th block is denoted as $_sZ_{ij}$, (i = 1,2,...,n). The longitudinal nominal strain increment of concrete at any point of the cross section is

$$\Delta_c\varepsilon_{ij} = \Delta\varepsilon_{0j} - Z_{ij}\,\Delta\phi_j \tag{11}$$

in which, ε_{0j} = normal strain at the member axis, x;ϕ_j = curvature of j-th block.

Bending moment ΔM_j^c and normal force ΔN_j^c in concrete are expressed by the following equations.

$$\Delta M_j^c = -\sum_{i=1}^{m} Z_{ij}\,A_{ij}\,\Delta_c\sigma_{ij} + \sum_{i=1}^{m} {}_cE_{ij}\,I_{ij}\,\Delta\phi_j \tag{12}$$

$$N_j^c = \sum_{i=1}^{m} A_{ij}\,\Delta_c\sigma_{ij} \tag{13}$$

where, A_{ij} = area of concrete in i-th layer of j-th element, and $\nabla_c\sigma_{ij}$ = normal stress in the concrete in the longitudinal direction in i-th layer of j-th block element. I_{ij} = moment of inertia of i-th layer about centroidal axis of its layer.

Similar expressions for reinforcements can be obtained as follows:

$$\Delta M_j^s = -\sum_{i=1}^{n} {}_sA_{ij}\,{}_sZ_{ij}\,\Delta_s\sigma_{ij} \tag{14}$$

$$\Delta N_j^s = \sum_{i=1}^{n} {}_sA_{ij}\,\Delta_s\sigma_{ij} \tag{15}$$

On the other hand, normal stresses in concrete

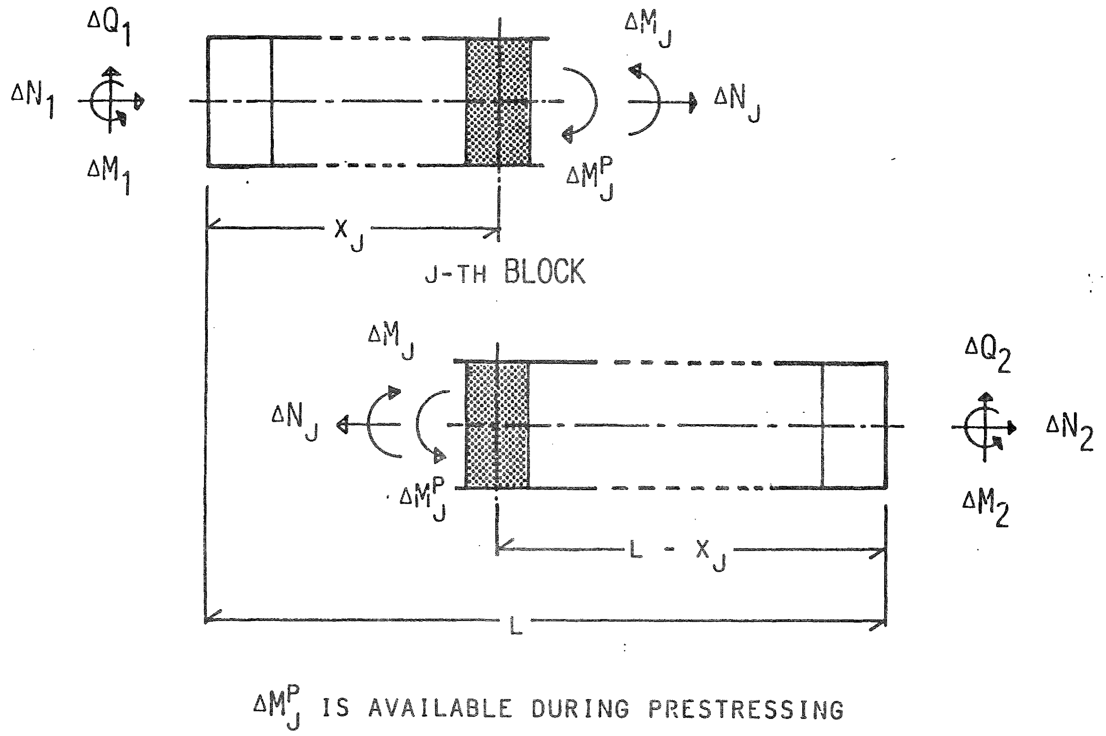

FIGURE 3 - EQUILIBRIUM OF FORCES OF THE MEMBER

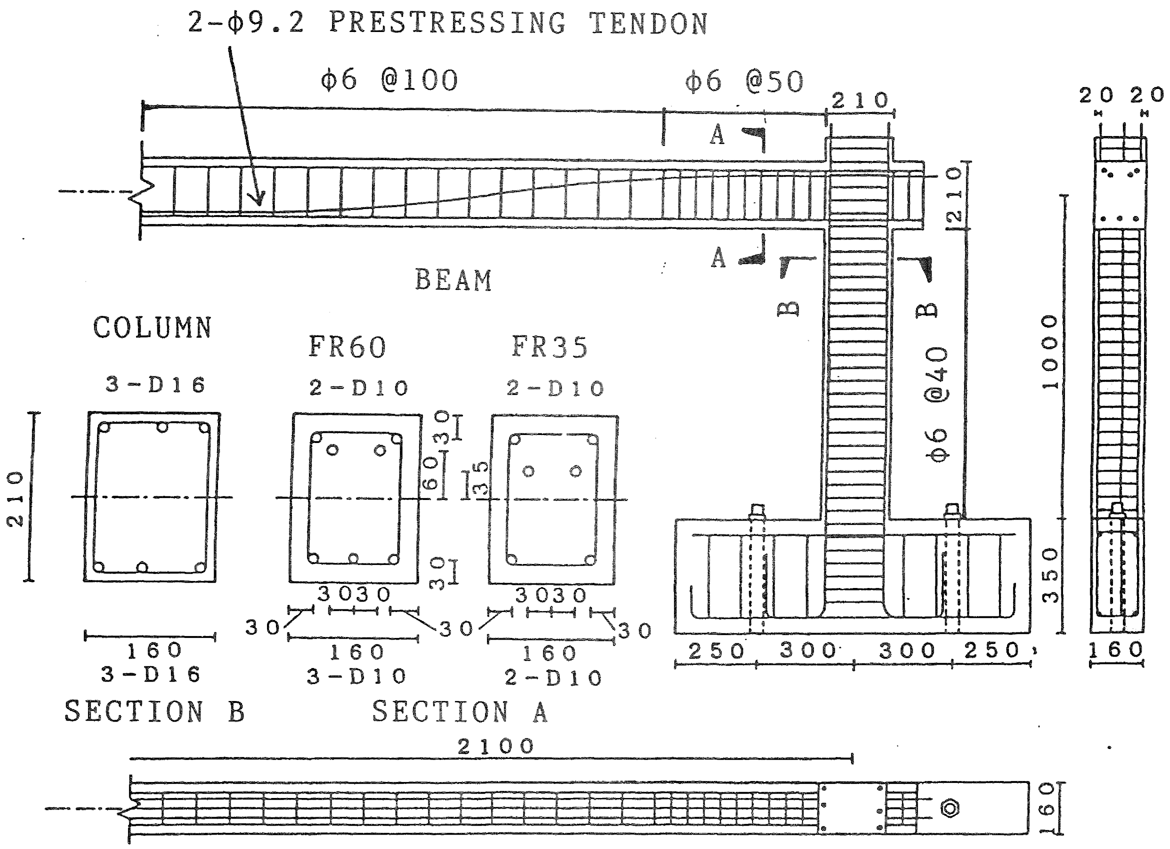

FIGURE 4 - DIMENSIONS AND REINFORCING DETAILS OF SPECIMEN

and reinforcement are expressed by the following equations.

$$\Delta_c\sigma_{ij} = {}_cE_{ij}\,\Delta_c\varepsilon_{ij} = {}_cE_{ij}(\Delta\varepsilon_{0j} - Z_{ij}\Delta\phi_j) \tag{16}$$

$$\Delta_s\sigma_{ij} = {}_sE_{ij}\,\Delta_s\varepsilon_{ij} = {}_sE_{ij}(\Delta_c\varepsilon_{ij} - \Delta_b\varepsilon_{ij}) \tag{17}$$

${}_cE_{ij}$, ${}_sE_{ij}$ = tangent modulus of concrete and longitudinal steel. Substituting Eqs. 16 and 17 into Eqs. 12-15, this yields,

$$\Delta M_j^c = \left[\sum_{i=1}^{m}(-Z_{ij}\,A_{ij}\,{}_cE_{ij})\right]\Delta\varepsilon_{0j} + \left[\sum_{i=1}^{m}{}_cE_{ij}(A_{ij}\,Z_{ij}^2 + I_j)\right]\Delta\phi_j \tag{18}$$

$$\Delta N_j^c = \left[\sum_{i=1}^{m}{}_cE_{ij}\,A_{ij}\right]\Delta\varepsilon_{0j} + \left[\sum_{i=1}^{m}(-\,{}_cE_{ij}\,A_{ij}\,Z_{ij})\right]\Delta\phi_j \tag{19}$$

$$\Delta M_j^s = \left[\sum_{i=1}^{n}{}_sZ_{ij}\,{}_sE_{ij}\right]\Delta\varepsilon_{0j} + \left[\sum_{i=1}^{n}{}_sE_{ij}\,{}_sA_{ij}\,{}_sZ_{ij}^2\right]\Delta\phi_j \tag{20}$$

$$\Delta N_j^s = \left[\sum_{i=1}^{n}{}_sA_{ij}\,{}_sE_{ij}\right]\Delta\varepsilon_{0j} + \left[\sum_{i=1}^{n}(-\,{}_sE_{ij}\,{}_sA_{ij}\,{}_sZ_{ij})\right]\Delta\phi_j \tag{21}$$

The total forces ΔN_j and ΔM_j in the cross section are obtained by summing up the contributions of concrete and steel. This yields

$$\Delta N_j = \Delta N_j^c + \Delta N_j^s = \alpha_j\,\Delta\varepsilon_{0j} + \beta_j\,\Delta\phi_j \tag{22}$$

$$\Delta M_j = \Delta M_j^c + \Delta M_j^s = \beta_j\,\Delta\varepsilon_{0j} + \gamma_j\,\Delta\phi_j \tag{23}$$

$$\alpha_j = \left[\sum_{i=1}^{m}{}_cE_{ij}\,A_{ij}\right] + \left[\sum_{i=1}^{n}{}_sA_{ij}\,{}_sE_{ij}\right] \tag{24}$$

$$\beta_j = \left[\sum_{i=1}^{m}(-\,{}_cE_{ij}\,A_{ij}\,Z_{ij})\right] + \left[\sum_{i=1}^{n}(-\,{}_sE_{ij}\,{}_sA_{ij}\,{}_sZ_{ij})\right] \tag{25}$$

$$\gamma_j = \left[\sum_{i=1}^{m}{}_cE_{ij}(A_{ij}\,Z_{ij}^2 + I_{ij})\right] + \left[\sum_{i=1}^{m}{}_sE_{ij}\,{}_sA_{ij}\,{}_sZ_{ij}^2\right] \tag{26}$$

Eqs. 23 and 24 represent the force-deformation relations for a cross-section of the beam. When Eqs. 23 and 24 are rewritten in the matrix form, this provides

$$\begin{Bmatrix}\Delta N_j\\ \Delta M_j\end{Bmatrix} = \begin{bmatrix}\alpha_j & \beta_j\\ \beta_j & \gamma_j\end{bmatrix}\begin{Bmatrix}\Delta\varepsilon_{0j}\\ \Delta\phi_j\end{Bmatrix} \tag{27}$$

Consideration of Prestress

From the equilibrium of forces shown in Fig. 3, the increments of axial force and bending moment in j-th block, ΔN_j and ΔM_j are obtained as follows.

$$\Delta N_j = \Delta N_2 = -\,\Delta N_1 \tag{28}$$

$$\Delta M_j = \Delta Q_2(1-{}_{x_j}) + \Delta M_2 + \Delta M_j^p$$

$$= -\Delta M_1 + x_j\,\Delta Q_1 + \Delta M_j^p \tag{29}$$

where, ΔN_1, ΔQ_1 and ΔM_1 = axial force and moment at the end 1 of the member, and $\Delta M_j p$ = moment induced by the prestress transfer, given by $\Delta Np\cdot ej$, where ΔNP = effective prestressing force, ej = eccentricity of tendon measured from the centroidal axis of the section. That is, prestress, which is divided into some loading steps, is assumed to be applied to each block as external loads ΔN_p and $\Delta M_j p$. During prestressing, tendons are not considered as reinforcements but prestressing force is just replaced by the external loads ΔNp and $\Delta M_j p$. After prestress transfer, they are assumed to behave like nonprestressing reinforcements with yield strength of $\sigma y - \sigma_p$ in tension and $-\sigma y - \sigma_p$ in compression, where σy = nominal yield stress of prestressing tendon and σ_p = effective prestress.

Derivation of the Stiffness Matrices of the Member and the Structure

The stiffness matrices of the member and the structure were constituted by the procedure presented by Kosaka et al. [3] and Tani et al. [6]. The effect of prestress is included in the terms due to bond-slip and nonlinearity of material properties.

Computational Algorithm

The computational algorithm in each loading step may proceed as follows:

1. For all elements, assume that $\Delta\varepsilon_{0j}$ and $\Delta\phi_j$ are the same as in the previous step.
2. Set up the bond stiffness equation in which the bond stiffness and the tangential modulus of reinforcement are assumed to be the same as in the previous step.

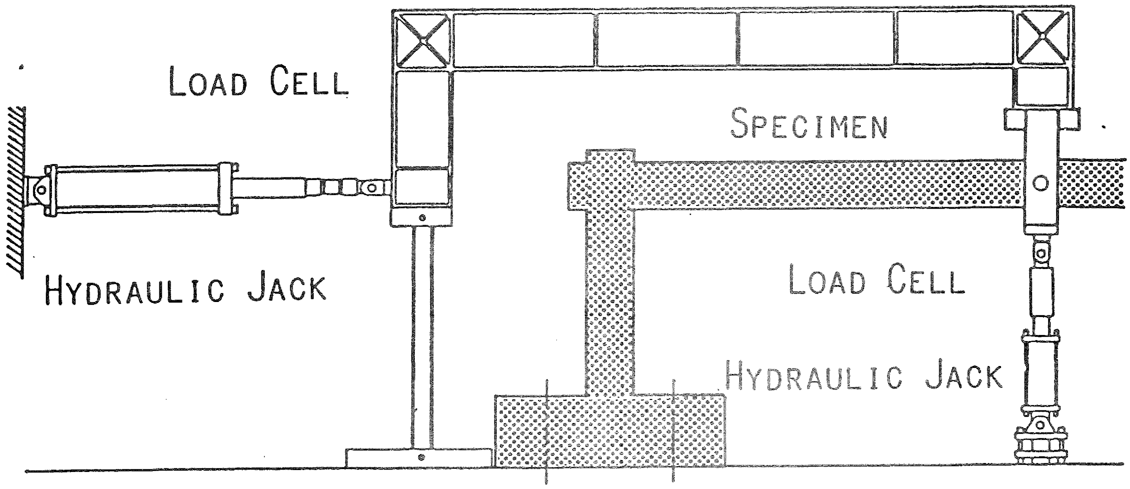

FIGURE 5 - LOADING SET-UP

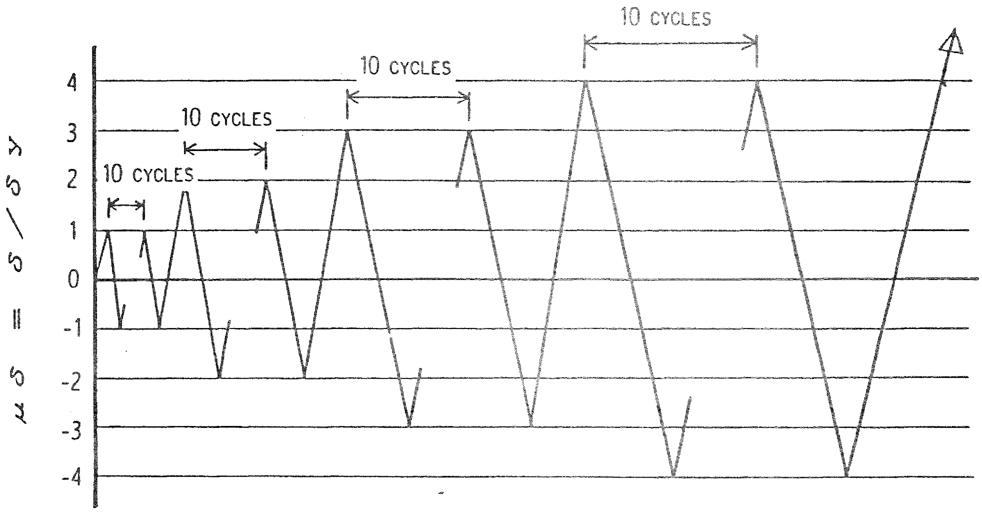

FIGURE 6 - IMPOSED LOADING HISTORY ON THE SPECIMEN

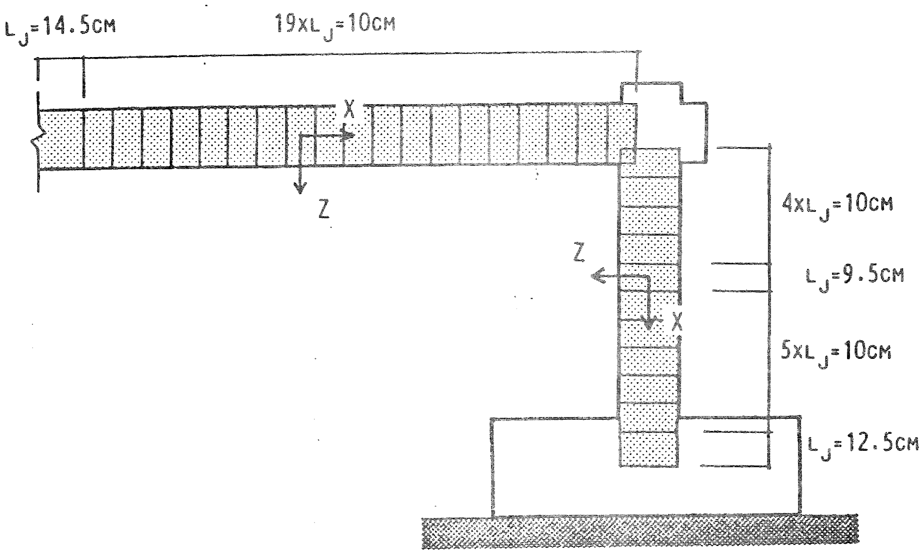

FIGURE 7 - DIVIDED BLOCK ELEMENTS OF THE MEMBER USED IN THE CALCULATION

3. Solve the equation above to get the slip between concrete and reinforcement in each block.
4. Set up the stiffness matrix of each block and transfer it into the flexibility matrix.
5. Combine the flexibility matrices of the sections so that the member flexibility matrices can be obtained.
6. Transfer the member flexibility matrices into the stiffness ones and constitute the stiffness matrix of the structure.
7. Solve the equation above under some support conditions and get the unknown displacements and forces.
8. Calculate $\Delta\varepsilon_{0j}$ and $\Delta\phi_j$ again by using the displacement and force increments obtained above.
9. Compare the assumed values and calculated values of $\Delta\varepsilon_{0j}$ and $\Delta\phi_j$, and return to step 1 if the difference between them is larger than one percentage of the assumed values. If not, go next.
10. Calculate the stresses and tangential modulus of concrete and reinforcement according to the strains obtained by using $\Delta\varepsilon_{0j}$ and $\Delta\phi_j$. If the tangential modulus in this step differs from the assumed value, unequivalent stress is calculated and released in the next step.

EXPERIMENT OF UNBONDED PRESTRESSED CONCRETE PORTAL FRAME

For verifying the propriety of the analytical method above, the experiment was carried out on two portal frames with an unbonded prestressed concrete beam 4.2 m long and reinforced concrete columns 1 m high, shown in Fig. 4. These two frames were so designed as to have the same lateral load resistance. The mechanical properties of concrete and reinforcement are listed in Tables 1 and 2. Specified 0.2% offset yield strength and tensile strength of prestressing tendon are 1078 MPa and 1225 MPa, respectively. The moment capacity of the column is about 1.5 times that of the beam, so that the plastic hinges are intended to be located in beam ends and column bases. One frame, 'FR35', was consisted of the beam where the eccentricity of prestressing tendon is 35 mm (D/6:D indicates the whole depth) and the other, 'FR60', has the prestressing tendon whose eccentricity is 60 mm (D/3.5). Effective prestresses are 107.8 kN for FR35 and 63.7 kN for FR60.

TABLE 1 - MECHANICAL PROPERTIES OF CONCRETE

Specimen	FR35	FR60
Compressive Strength f'_c in MPa	36.9	36.8
Strain at f'_c in %	0.244	0.218
Tensile Strength f_t in MPa	3.4	3.3

TABLE 2 - MECHANICAL PROPERTIES OF REINFORCEMENTS

Reinforcement	D10	D16	ϕ6
Yield Strength f_y in Mpa	350.6	346.3	395.9
Yield Strain ε_y in %	0.205	0.180	0.224
Modulus of Elasticity in 10^5 MPa	1.72	1.92	1.76

Prestress was transferred to the beam while one column base is supported by pin and the other is supported by roller. Therefore, the columns were free from the moments, shears and axial forces produced by prestressing. After prestress transfer, the frame was fixed to the floor. This procedure was followed in the calculation, but the friction of tendon during prestress transfer is ignored.

Fig. 5 shows loading set-up. Reversed cyclic horizontal load was statically applied to the mid-span of the beam by hydraulic jack. Besides the horizontal load, the vertical load was also applied at the mid-span of the beam, so that the bending moments at the beam ends and the mid-span due to the prestressing were offset at the beginning of the test. This vertical load was kept constant during the test.

The frames were subjected to several slow load reversals simulating very severe earthquake loading. The 'first yield' displacement of the frames were found when all the tension reinforcements in expected hinging regions had yielded. The first loading cycle consisting of ten cycles was followed by a series of deflection controlled cycles in the inelastic range, also comprising ten full cycles to each of the displacement ductility factors of ±2, ±3, ±4, and sometimes higher, as illustrated in Fig. 6.

In the calculation bond stiffness assumed for prestressing tendon is 9.8 x 10^3 N/mm^3. This is about 1/1000 used for nonprestressed deformed bar. Fig. 7 shows layer elements assumed in the calculation.

EXPERIMENTAL RESULTS AND COMPARISON WITH THE ANALYTICAL RESULTS

Figs. 8 and 9 show the first cycle in each series of deflection cycles of the measured horizontal load versus horizontal deflection at the midspan of the beam. These figures also show the calculated load - deflection curves. The deterioration due to load cycles in concrete and bond is not considered in this calculation, so that each loading cycle comprises only one full cycle. When the experimental results are compared with analytical results, fairly good agreement can be observed.

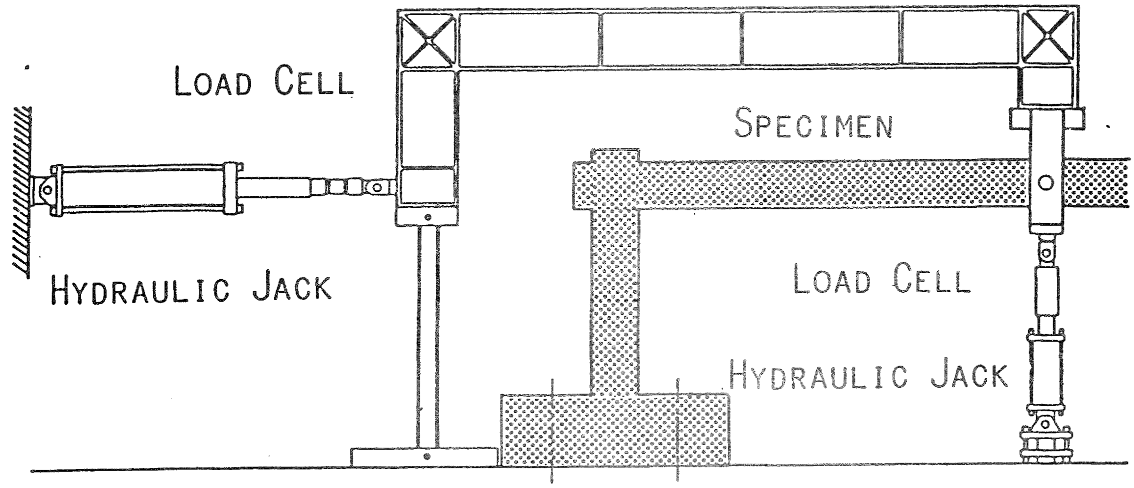

FIGURE 5 - LOADING SET-UP

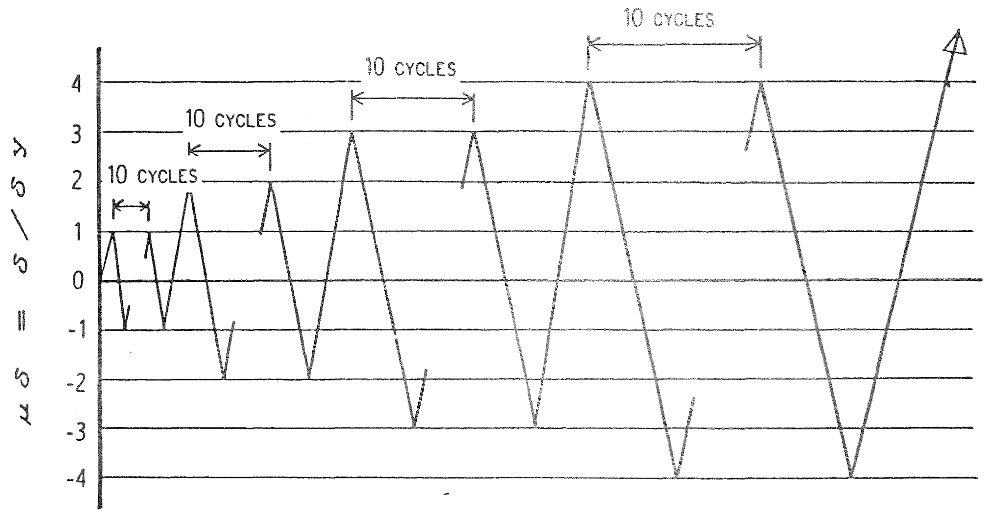

FIGURE 6 - IMPOSED LOADING HISTORY ON THE SPECIMEN

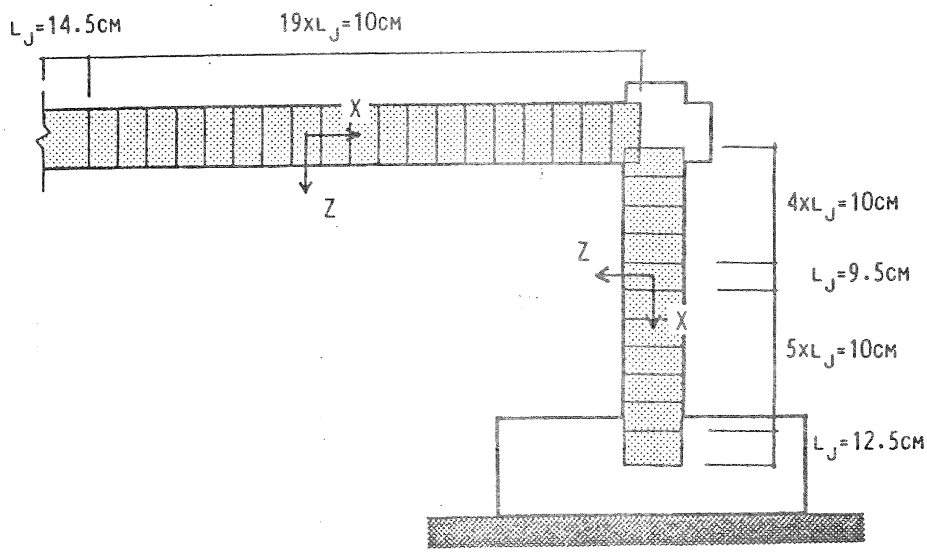

FIGURE 7 - DIVIDED BLOCK ELEMENTS OF THE MEMBER USED IN THE CALCULATION

3. Solve the equation above to get the slip between concrete and reinforcement in each block.
4. Set up the stiffness matrix of each block and transfer it into the flexibility matrix.
5. Combine the flexibility matrices of the sections so that the member flexibility matrices can be obtained.
6. Transfer the member flexibility matrices into the stiffness ones and constitute the stiffness matrix of the structure.
7. Solve the equation above under some support conditions and get the unknown displacements and forces.
8. Calculate $\Delta\varepsilon_{0j}$ and $\Delta\phi_j$ again by using the displacement and force increments obtained above.
9. Compare the assumed values and calculated values of $\Delta\varepsilon_{0j}$ and $\Delta\phi_j$, and return to step 1 if the difference between them is larger than one percentage of the assumed values. If not, go next.
10. Calculate the stresses and tangential modulus of concrete and reinforcement according to the strains obtained by using $\Delta\varepsilon_{0j}$ and $\Delta\phi_j$. If the tangential modulus in this step differs from the assumed value, unequivalent stress is calculated and released in the next step.

EXPERIMENT OF UNBONDED PRESTRESSED CONCRETE PORTAL FRAME

For verifying the propriety of the analytical method above, the experiment was carried out on two portal frames with an unbonded prestressed concrete beam 4.2 m long and reinforced concrete columns 1 m high, shown in Fig. 4. These two frames were so designed as to have the same lateral load resistance. The mechanical properties of concrete and reinforcement are listed in Tables 1 and 2. Specified 0.2% offset yield strength and tensile strength of prestressing tendon are 1078 MPa and 1225 MPa, respectively. The moment capacity of the column is about 1.5 times that of the beam, so that the plastic hinges are intended to be located in beam ends and column bases. One frame, 'FR35', was consisted of the beam where the eccentricity of prestressing tendon is 35 mm (D/6:D indicates the whole depth) and the other, 'FR60', has the prestressing tendon whose eccentricity is 60 mm (D/3.5). Effective prestresses are 107.8 kN for FR35 and 63.7 kN for FR60.

TABLE 1 - MECHANICAL PROPERTIES OF CONCRETE

Specimen	FR35	FR60
Compressive Strength f'_c in MPa	36.9	36.8
Strain at f'_c in %	0.244	0.218
Tensile Strength f_t in MPa	3.4	3.3

TABLE 2 - MECHANICAL PROPERTIES OF REINFORCEMENTS

Reinforcement	D10	D16	ϕ6
Yield Strength f_y in Mpa	350.6	346.3	395.9
Yield Strain ε_y in %	0.205	0.180	0.224
Modulus of Elasticity in 10^5 MPa	1.72	1.92	1.76

Prestress was transferred to the beam while one column base is supported by pin and the other is supported by roller. Therefore, the columns were free from the moments, shears and axial forces produced by prestressing. After prestress transfer, the frame was fixed to the floor. This procedure was followed in the calculation, but the friction of tendon during prestress transfer is ignored.

Fig. 5 shows loading set-up. Reversed cyclic horizontal load was statically applied to the mid-span of the beam by hydraulic jack. Besides the horizontal load, the vertical load was also applied at the mid-span of the beam, so that the bending moments at the beam ends and the mid-span due to the prestressing were offset at the beginning of the test. This vertical load was kept constant during the test.

The frames were subjected to several slow load reversals simulating very severe earthquake loading. The 'first yield' displacement of the frames were found when all the tension reinforcements in expected hinging regions had yielded. The first loading cycle consisting of ten cycles was followed by a series of deflection controlled cycles in the inelastic range, also comprising ten full cycles to each of the displacement ductility factors of ±2, ±3, ±4, and sometimes higher, as illustrated in Fig. 6.

In the calculation bond stiffness assumed for prestressing tendon is 9.8×10^3 N/mm^3. This is about 1/1000 used for nonprestressed deformed bar. Fig. 7 shows layer elements assumed in the calculation.

EXPERIMENTAL RESULTS AND COMPARISON WITH THE ANALYTICAL RESULTS

Figs. 8 and 9 show the first cycle in each series of deflection cycles of the measured horizontal load versus horizontal deflection at the midspan of the beam. These figures also show the calculated load - deflection curves. The deterioration due to load cycles in concrete and bond is not considered in this calculation, so that each loading cycle comprises only one full cycle. When the experimental results are compared with analytical results, fairly good agreement can be observed.

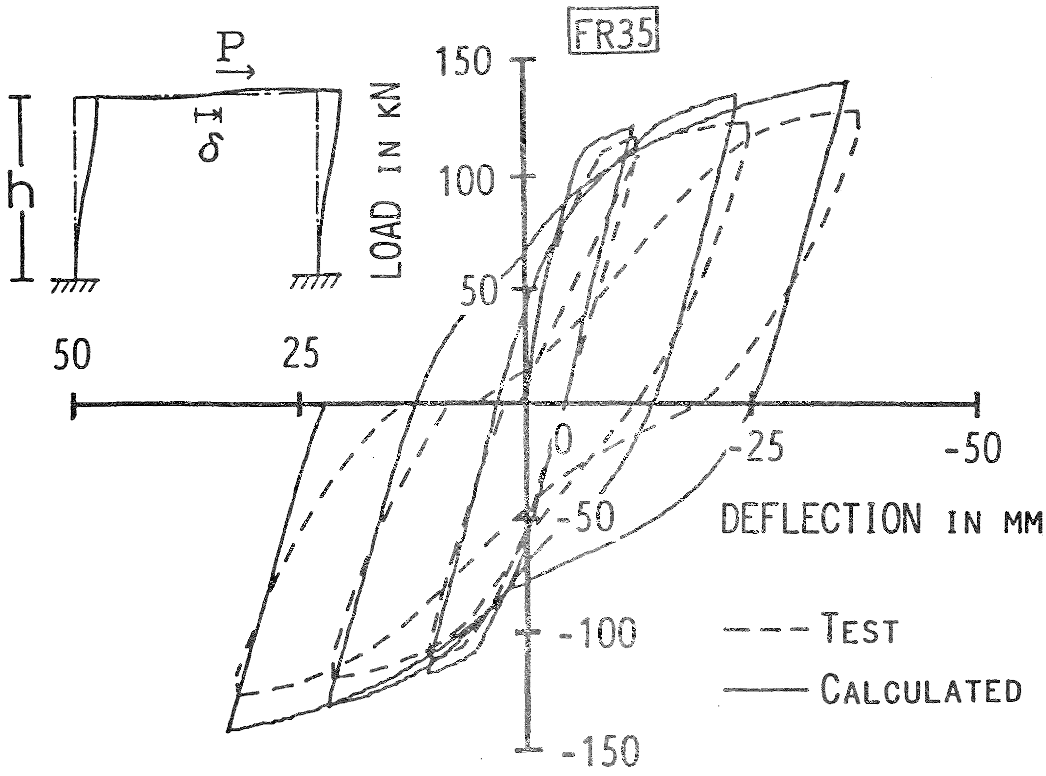

FIGURE 8 - LOAD - DEFLECTION RELATION IN FR35

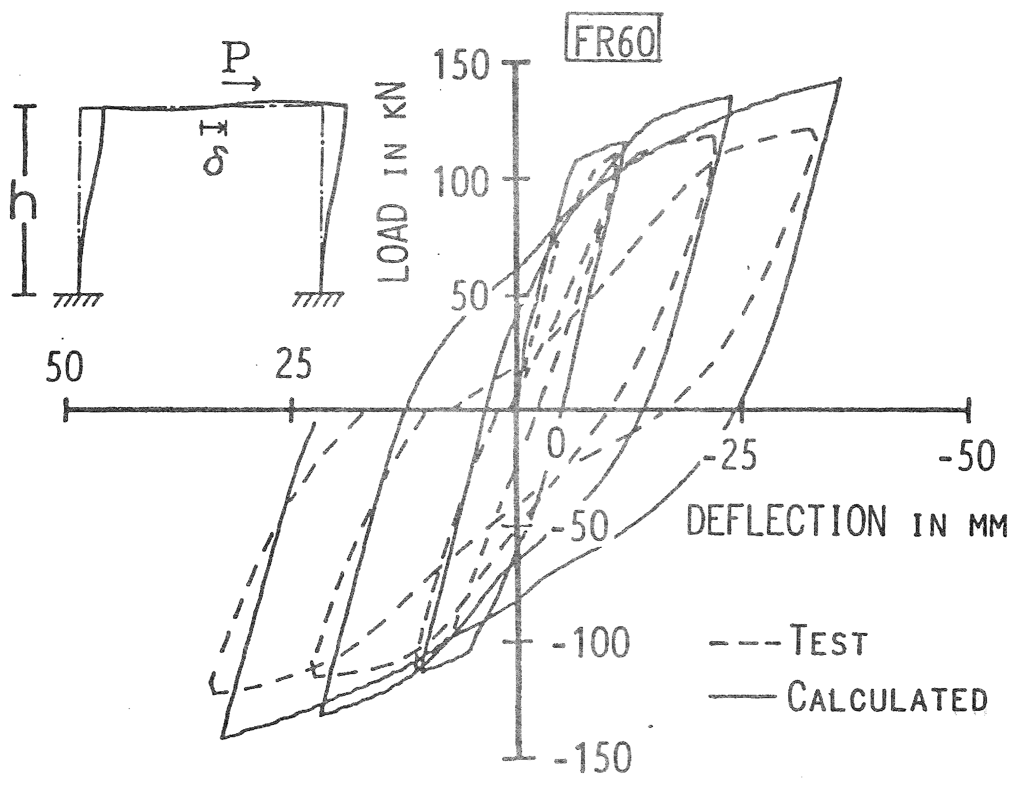

FIGURE 9 - LOAD - DEFLECTION RELATION IN FR60

However, the larger the deformation became, the larger difference could be observed. It is mainly because the shear deformation was not taken into consideration in the calculation. The shear deformation, especially in the column, dominates the whole deformation of the frame in the loading cycles to high ductility values, and some pinching of the load-deflection loops was noticeable in the experiment. Just before the failure, where the ductility factor is almost +4, the shear deformation of the column base occupies a large portion of the whole deformation, while the deformation of the beam remains small. Therefore, the frame moves like a rigid body connected to the foundation at the column base.

In Figs. 10 and 11, the first cycle in each series of deflection cycles of the measured tendon force increments versus horizontal deflections at the midspan of the beam are shown. The calculated results are also shown in the same figures. As described before, the shear deformation at the column bases results in imposing not so large rotation on the beam ends even in the inelastic range. Therefore, the calculated results are larger than the experimental results. In addition, in the calculation, the tendon force increment continues to increase almost linearly with the deflection of the frame because the rotations at the beam ends have a linear relationship with the lateral deflection of the frame.

The maximum tendon force increment measured in the test was up to 196 N/mm^2. From analytical and experimental results on the portal frame, the tendon force measured at the anchorage ends is not so large. It may be not necessary to consider any risk of tendon fracture even in the inelastic range. The tendon force increment measured in the test showed good agreement with the predicted value obtained from ACI and NZS.

CONCLUSIONS

The analytical method, by which hysteretic restoring force characteristics of unbonded prestressed concrete framed structures can be statically pursued on the basis of material properties, was presented. The analytical results were compared with the experimental results of unbonded prestressed concrete portal frame in terms of lateral load versus deflection and increment of tendon stress versus deflection relation. Fairly good agreement can be observed. However, the larger difference could be found in the loading cycles to high ductility values because the shear deformation became dominant. Therefore the method has to be so improved as to take inelastic shear deformation into consideration.

The analytical and experimental results showed that the tendon force was not so large because the rotation of the beam ends was not so large while the large inelastic deformation was imposed on the frame. Therefore, it may be not necessary to consider any risk of tendon fracture and the unbonded tendon will be successfully used in primarily earthquake resistant members.

REFERENCES

[1] Du, Gongchen and Tao, Xuekang 1985 Ultimate Stress of Unbonded Tendons in Partially Prestressed Concrete Beams, PCI Journal, Nov.-Dec.,72-91.

[2] Kent, D.C. and Park, R. 1971 Flexural Members with Confined Concrete, Proc. of ASCE, Vol.97, ST7, July.,1979-1990.

[3] Kosaka, Y., Tangiwa, Y. and Yamada, K. 1983 Inelastic Analysis of Reinforced Concrete Based on Endochronic Theory - Part 1 Procedure of Analysis - Transaction of the AIJ No. 326, April., 78-90 (in Japanese).

[4] Muguruma, H., Watanabe, F. and Shimizi, Y. 1982 Improving the Flexural Ductility of Post-tensioned Unbonded Beam by Using Laterally Confined Concrete, Proc., of JCI 4th Conference,361-364 (in Japanese).

[5] Park, R., Kent, D.C. and Sampson, R.A. 1972 Reinforced Concrete Members with Cyclic Loading, Proc. of ASCE, ST7, July, 1341-1360.

[6] Tani. S., Nomura, S., Nagasaka, T., and Hiramatsu, A. 1977 Restoring Force Characteristics of Reinforced Concrete Aseismic Elements (Part 4) - Pursuit of Restoring Force Characteristics by Means of a Static Elastic-Plastic Analytical Method. Transaction of the AIJ No. 262, Dec., 61-72.

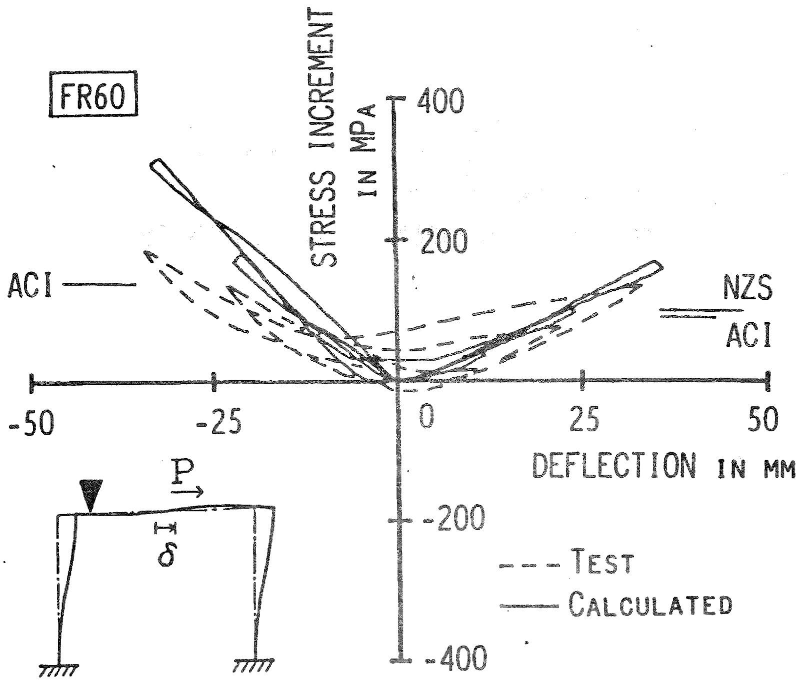

FIGURE 10 - INCREMENT OF TENDON STRESS - DEFLECTION RELATION IN FR 60

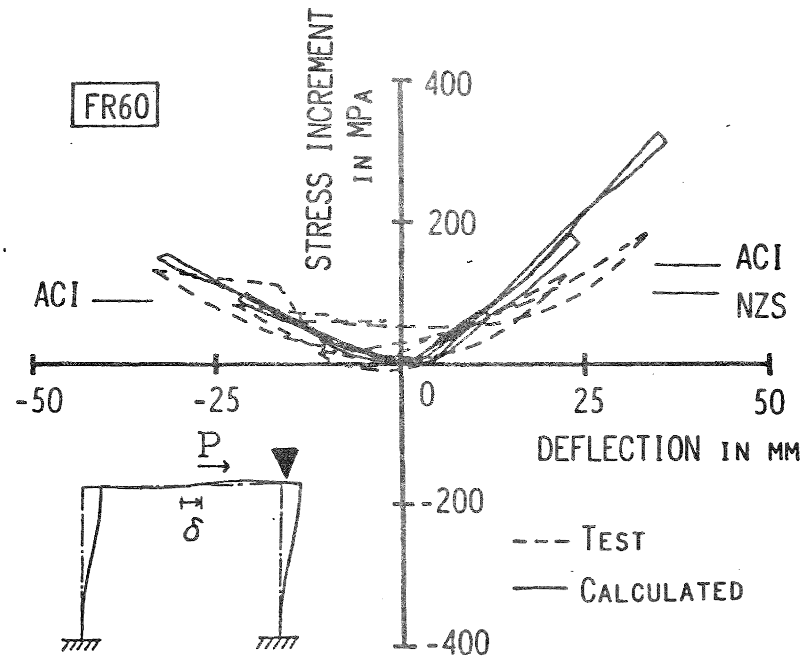

FIGURE 11 - INCREMENT OF TENDON STRESS - DEFLECTION RELATION IN FR60